A Real-time and Vision-based Methodology for Processing 3D Objects on a Conveyor Belt

Michael Weyrich, Martin Laurowski, Philipp Klein, and Yongheng Wang
Chair of Automated Manufacturing and Assembly
University of Siegen
Paul-Bonatz-Straße 9-11; 57068 Siegen
GERMANY
martin.laurowski@uni-siegen.de http://www.uni-siegen.de/fb11/lfa/

***Abstract*—**The objective of this paper is to present an industrial vision-based methodology for processing 3D objects being conveyed by a constant velocity. This methodology employs a camera system and a robotic system. The object on the conveyor is firstly captured by camera system. The geometry and texture of object are further estimated and analyzed, in order to indentify defective surface and its location with reference to the object geometry. These efforts are instructive to generate a path plan for processing defective objects, which is implemented by the robotic system. The strength of this methodology is to combine vision-based defect detection and automated path planning that make it flexible to objects with variant geometries without the expense of operation time. In food industry this methodology is competent to reduce wastes.

***Keywords*—**real-time, vision-based, optical inspection, 3D objects, conveyed objects, food industry, food processing, surface defects detection, geometry estimation, path planning

I. Introduction

VISION-based automated inspection is the main measure in industrial quality control. The approach is to sort objects or products according to vision features, which are predefined, into variant categories indicating different quality levels. Quality control of screw production is of the typical example. In food industry, vision-based automated inspection is also frequently employed. However, with the expectation of reducing waste, further processing is then implemented to the presorted food. Comparing for example to the screw production, the inspected objects in food industry are always inhomogeneous geometrical objects. Therefore, surface inspection and shape recognition have to be combined to sort out defective objects automatically. In addition to this, specific processing of defective objects helps reducing the waste. Therefore, the evaluation of the detected defects aims to deduce the processing path and method. Both have to be adapted to the inspected volumetric object and the industrial process.

Throughput is particularly important for the food processing industry. In order to achieve that the products consistently meet specified quality standards the quality control should be automated. The large amount of products and the increasing stress due to competition contribute to the demand for automated optical inspection in combination with specific processing of defective objects. Usually, the quality inspection is integrated within the production process. The industrial conditions, the irregular shape and the movement of the objects have to be considered to the testing system. The path planning and the processing method are deduced by the optical detected defects.

The objective of this paper is to present a vision based, automated path planning methodology for processing 3D objects on a conveyor belt (see Fig.1-1). This methodology involves a camera system used for 3D detection and an interactive path planning solution for a fixed-based manipulator from an initial to a final configuration. The desired path should possess two characters: collision-free and metric minimization.

Manuscript received April 8, 2011.
This work was funded by the European Fond for Regional Development and the government of north Rhine Westphalia under the reference number NA035D.

All authors are at the Chair of Automated Manufacturing and Assembly, University of Siegen, 57068 Siegen, Germany, e-mail: michael.weyrich@uni-siegen.de, martin.laurowski@uni-siegen.de, philipp.klein@uni-siegen.de, yongheng.wang@uni-siegen.de

II. State of the Art

A survey on methods for quality inspection of agricultural products reveals a wide variety of image based methods. References [1], [2], [3] and [4] describe the application of multispectral analysis for quality inspection. The analysis and processing of acquired images are described in [5]. Stereo vision image processing for moving objects is described in [6] and [7]. A fast and robust 3D localization method based on object edge is proposed in [8]. An approach for geometry acquisition on natural structures is proposed by [9] using a laser scanner. In [10] a geometry acquisition method by the time of flight principle is described. Further principles are stereo vision [11] and shape from shading [12]. A possibility to acquire the geometry and intensity information of an object simultaneously using a line scan camera setup is proposed in [13].

General approaches on active stereo vision are evaluated in [14] and [15]. A matching method using structured light in order to improve the precision and efficiency of 3D measurement is proposed in [16]. Reference [17] describes an accurate hardware-based stereo vision. A 3D measurement method based on mesh candidate and structured light for online depth recovery is described in [18]. An approach for shape classification of objects is proposed in [19]. For classification of image features following approaches can be used: decision trees, support vector machines (SVM), neuronal networks and k-nearest neighbor. According to the research results proposed in [20], a combination of k-nearest neighbor with SVM is recommended for the visual surface inspection.

Defects in agricultural products are mentioned in [21]. A classification of cutting methods to correct defects in agricultural products is described in [22].

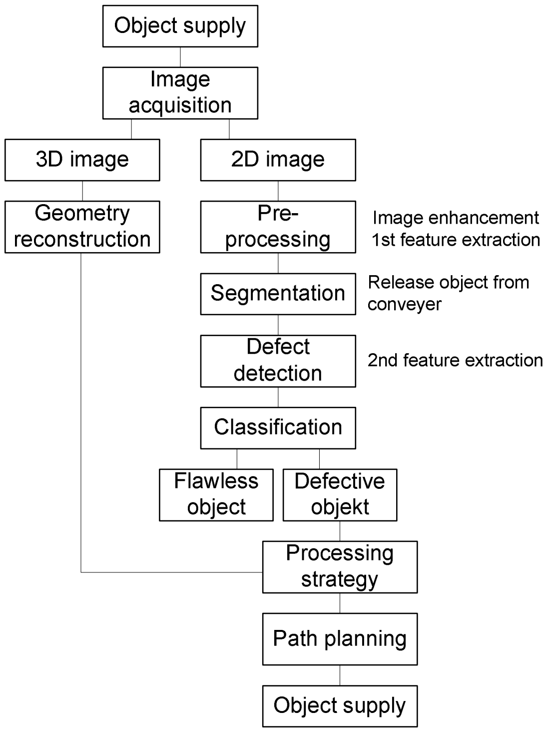

Figure 1-1: Information flow of an automated optical inspection and processing system

III. Appoach for Defects Detection and Shape Recognition

Imaging of the object to inspect can be divided in two main sub tasks – surface imaging and geometry estimation. Principally, there are many approaches in the field of optical inspection methods to perform the automated optical inspection systems. According to a given task a suitable combination of methods should be selected. Commonly used approaches combinations have been systemized and evaluated (Table 3-1).

In the field of optical surface inspection improving of contrast between the defective and flawless area of an object plays a major role for reliable and stable automated detection processes. The contrasting is defined especially in terms of lighting and optics.

In the field of geometry estimation the shape and dimensions of the object to inspect have to be known in order to describe the location of defect. Finally, the defective area can be automatically processed by a machining system.

characteristic feature	***implementation options***						
camera technology	matrix camera			line scan camera			
number of cameras	1	2	3	4	5	...	n
surface acquisition mode	single image		multiple images		continuous		
relative movement	no movement		continuous		incremental		
light path between imaging sensor & object	direct	indirect					
		plane mirror	connical	spherical mirror	2-mirrors	...	n-mirrors
lens optics	entocentric		telecentric		hypercentric		
alignment object axis vs. camera axis	axial		radial		inclined		
parts feeding	linear		circular		free fall		

Table 3-1: Morphological analysis – characteristic features of an imaging system for automated inspection

A. Surface Defects Detection

In order to select an optimal method to image the object, different bands of the electromagnetic radiation have to be analyzed. Systematic experiments with different imaging techniques should prove which approach satisfies the requirements.

Samples of materials to be tested are examined with a multispectral camera. The used multispectral camera allows imaging in the wavelength range of 450-950 nm. Band selections are performed by build in electronically controlled liquid crystal tunable filters (LCTF). Selective band image capture is possible with a bandwidth of 10 nm. Illumination of the test specimen is provided by a lighting setup with diffusers. Light sources are here halogen lamps. They radiate in a wide visible and infrared spectrum which corresponds with the sensitivity range of the multispectral camera. Optical band-pass filters and a conventional industrial camera can be used for the experiments as well.

Some of the defects types on agricultural products show characteristic features in particular wave lengths. Surface defects on an example of a potato tuber can be imaged with an best possible contrast in the wave length of 530-540 nm. Typical plots of intensity and contrast on a potato tuber over the wave length, acquired with a multispectral camera are shown in Fig. 3-1.

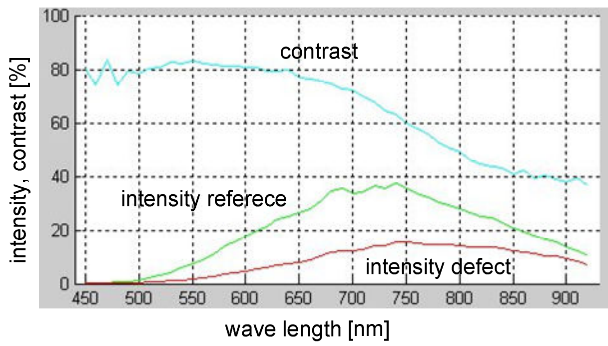

Figure 3-1: Intensity and contrast as function of the wave length acquired with a multispectral camera on a potato tuber.

In general, the near infrared band ($\lambda > 800$ nm) is suitable for visualizing of bigger and sub superficial positioned defects. With increasing weave length superficial defects disappear in images – only gross defect are visible (Fig. 3-2). This effect can be especially useful on agricultural products like apples which have irregular and changing surface colors.

Most of the surface defects on the tested specimens are superficial with a depth of approximately 0.3 mm. In order to realize a customized inspection system the specimen is illuminated with a custom made LED-lighting setup with 540 nm central wave length.

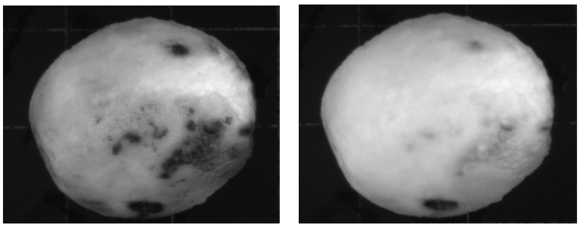

Figure 3-2: Surface defects on a potato tuber imaged in a spectral band 530-540 nm (left) and 900-910 nm (right).

The reflected light is received by a grey scale CCD image sensor and interpreted as brightness values. A color sensor or a multispectral imaging sensor arrangement can be used for special purposes as well. When selecting a customized light source with a particular wave length the spectral sensitivity of camera sensor should be considered (Fig. 3-3).

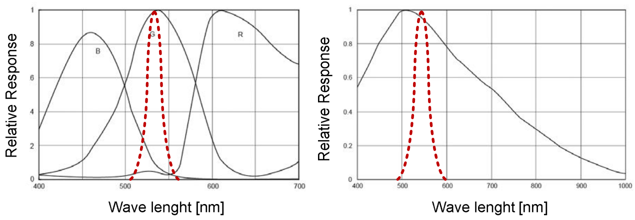

Figure 3-3: Spectral characteristic of a color camera sensor (left) and a gray scale sensor (right) with overlayed spectrum characteristic of an LED with 540nm centre wave length.

Due to changing requirements on the inspection task and products to inspect, the imaging and lighting systems have to be customized. A mobile image acquisition appliance helps to specify the defects on objects and their characteristic properties. The appliance (Fig. 3-5) consists of a multi spectral camera, conventional grey scale camera as well as different types of lightings and optical filters. During the preliminary tests a concept for customized imaging system can be tested under reference conditions.

In the following step the optimized imaging system can be configured and assembled.

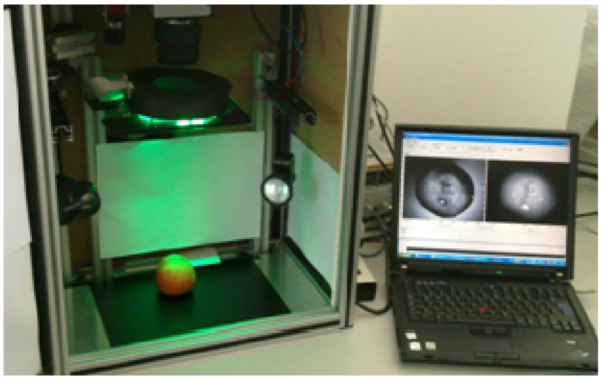

Figure 3-5: Mobile image acquisition appliance with various cameras and illumination sources.

B. *Geometry Estimation and Defects Localization*

Once the visual system for imaging the defects is selected the next task is to localize them geometrically in relation to the world coordinate system.

Estimation of the 3D object geometry has to be performed contact-free due to hygienic constrains. For further considerations optical systems based on following principles have been selected and experimentally analyzed:

- Photometric stereo (PS)
- Time-of-flight camera (TOF)
- Triangulation with structured light
- Stereo vision (SV)

Photometric Stereo

This principle is based on a 3D geometry reconstruction from different lighting conditions using a single camera. In some publications this principle is described as shape from shading (SFS).

The reachable depth and lateral resolution is satisfying. But due to natural irregular form, color and especially brightness deviations of agricultural products, test results were unfavorable. In many cases surface defects cause misinterpretations in depth estimation.

Time-of-Flight Camera

This type of camera uses modulated pulsed infrared light source and reconstructs the depth data from the time-of-flight. The image capturing works independent of the object surface color and brightness in terms of shape recognition but the achievable resolution does not meet the requirements. Current cameras provide a relative low resolution (lateral resolution: 200x200 pixel, depth resolution: approx. 10 mm).

Triangulation with Structured Light

The geometry estimation is here based on a matrix camera and a line laser module. This technique is similar to the light sheet principle. The achievable lateral and depth resolution is much better than the task requirements. To capture the whole object geometry a relative movement between the camera and object is necessary. A sequence of images is necessary in order to capture the object and reconstruct the object geometry. This property causes difficulties in image registration process.

Stereo Vision

The 3D information of an object is here reconstructed from a stereo camera setup and an unstructured light source (passive stereo vision). The geometry reconstruction process is based on disparity of particular image points. Textured surfaces improve the performance and accuracy of this process. Once the surface texture is missing or insufficient an artificial pattern can be projected on the surface (active stereo vision).

All the mentioned methods for object geometry capturing are capable to image a section of the geometry only. It is caused by the limited field of view from observing point and occlusion effects. In order to obtain a complete object topology the imaging systems have to be extended by more points of view and hence more cameras have to be used.

The choosing of imaging systems is a tradeoff among costs, accuracy, robustness, and so on. Practical experiments with selected imaging systems have been performed and evaluated in order to established requirements. The experiments results are represented in a radar diagram in Fig. 3-6.

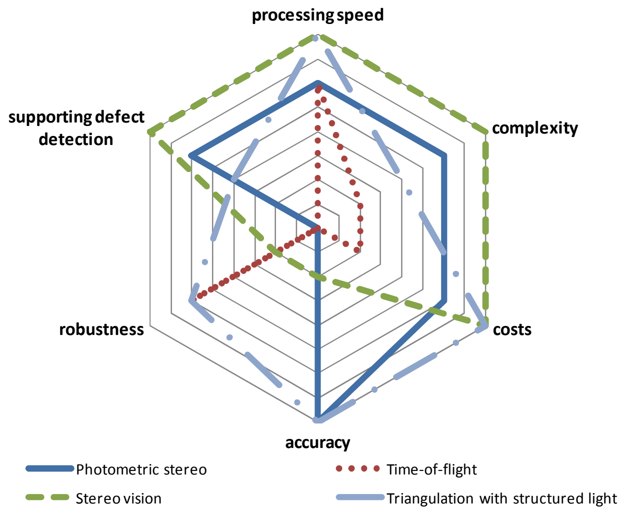

Figure 3-6: Comparison of principles for geometry estimation

Implementation

Comparison of experiment results lead to a choice for object geometry estimation using stereo vision with auxiliary pattern projection. Additional benefit is the possibility to acquire the geometry as well as the intensity images for surface inspection using the same camera setup.

An experimental system was developed consisting of two stereo modules. A stereo module consists of two single monochrome area scan cameras with entocentric lenses and a laser pattern generator. The optical axes are oriented toward the part under examination and are approximately antiparallely aligned. The parallax angle and the base line of a stereo module are adjusted to 6° (Fig. 3-7). The lenses are selected in order to cover the measurement volume. The cameras work with ½`` CCD sensors with a resolution of 752x582 pixel, global shutter and a maximal image rate of 49 frames per second. In correlation with the sensor size, entocentric lenses with a focal length of f=8.5 mm each have been applied.

In order to project a laser pattern on the surface collimated laser modules with a wavelength of λ=638 nm and a power of 30 mW have been used. The laser beam provides sufficient contrast to the surface of the test objects and can be detected well on the part to be inspected. The grid pattern of 51x51 rectangular lines is generated with a diffractive optical element (DOE) and has a fan angle of approx. 23°. Corresponding to the requirements on feeding speed to capture the object during a movement at the same position and same time, we use a camera trigger provided by an external sensor.

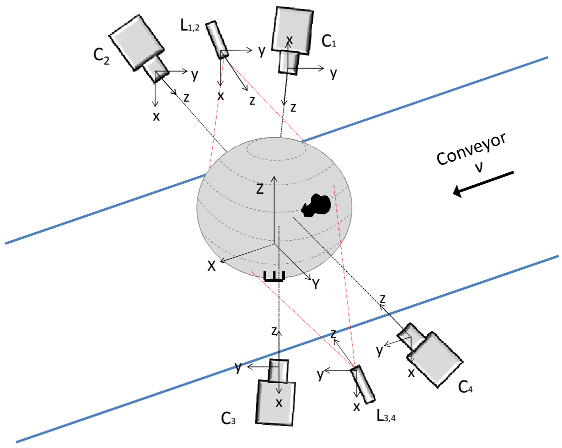

Figure 3-7: Imaging setup for geometry estimation and defects detection

The customized LED lighting systems for defects detection with a light wave length of 540 nm are mounted coaxially with cameras. To avoid the negative impact of visible grid pattern on images for surface defects detection a second set of images is needed. During the acquisition of geometry information only the pattern projectors are activated, the lighting system for surface defects is switched off. During acquisition of intensity images the LED lighting system is activated while the laser modules are switched off. While acquiring the second set of images the inspected object usually moves along the conveyor system. Due to a high frame rate of the cameras there is a relatively slight object displacement between both snapshots. It is corrected by an algorithm while matching the position of a surface defect in a 2D image with the 3D object model.

The projected grid pattern allows a significant improvement in performance of stereo images registration especially on sparse textured surfaces. To obtain the object geometry two pairs of stereo camera setups are used for the reconstruction. Partial views with visible laser pattern are shown in Fig. 3-8.

Various data processing steps are necessary in order to reconstruct the object shape from multiple views. Starting with the object image in the first step an image rectification is performed followed by correspondence analysis. The resulting disparity maps are filtered in order to remove the outliers. The following triangulation transforms the pixel oriented depth information in real world dept coordinate system. In the following step, the obtained point clouds are concatenated to a contiguous point cloud. This is performed by transformation of all partial point clouds into a common reference coordinate system.

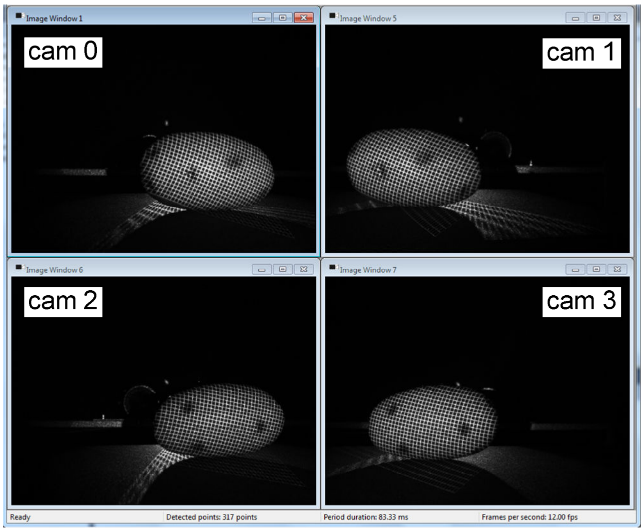

Figure 3-8: Four partial camera views of a potato tuber with projected grid pattern.

A mesh model is generated from the point cloud in the subsequent meshing process. This model includes usually some areas where the depth information is not available. These areas are closed by an appropriate reconstruction method in means of data interpolation (Fig. 3-9). The intensity values from the 2D image are mapped to the generated mesh. Thereby the texture information of the object can also be processed.

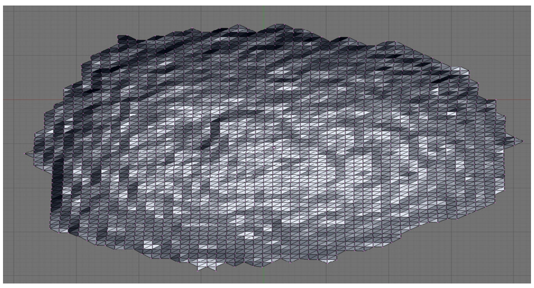

Figure 3-9: Mesh model with closed surface generated from a point cloud

Feature Extraction and Classification

Up to now, image acquisition and geometry estimation according different inspection requirement have been discussed. In the following, feature extraction and further classification will be presented.

Acquire image is only a record of light reflection of object (regarding to CCD, CMOS sensors), this means, not all image data are needed to analyzed, for example, back ground etc.. Once the optimal image of object is acquired, the next significant issue is to extract features, which transfers and reduces the input data (i.e. image) into a set of features (i.e. features vector). What can be a defect on the object surface? Fuß [23] has already categorized different types of surface defects (Table 3-2).

Classification of defect types	***Different feature***
	Local or global deviation
Color defect	Hue, intensity, sheen
Deviation of surface structure	Structure element: Shape, Size, Color, Orientation Arrangement of structure element: Size distribution, Distance, orientation
	Local deviation
Local, 3-dimensional distinct shape deviation	Characteristic on surface: point-shaped, 1-dimensional shaped, 2-dimensional shape Characteristic in depth: rise, deepening

Table 3-2: Classification scheme for surface defect [18]

In food industry, the investigated objects always have variant geometries, shapes, even textures. Therefore the second defect type, which is detected by defect shape, is not so frequent. Fig. 3-10 shows the two typical types of defect. What feature and which level of feature should be extracted is the first question in feature extraction. This should be accommodated to specific requirement. For instance, in this paper, the contour of object is needed to grasp, in order to extract the object as Region of Interest (ROI) from background. Then, within the ROI, the object texture is analyzed by utilizing the information of color or intensity variation, size of defect etc.

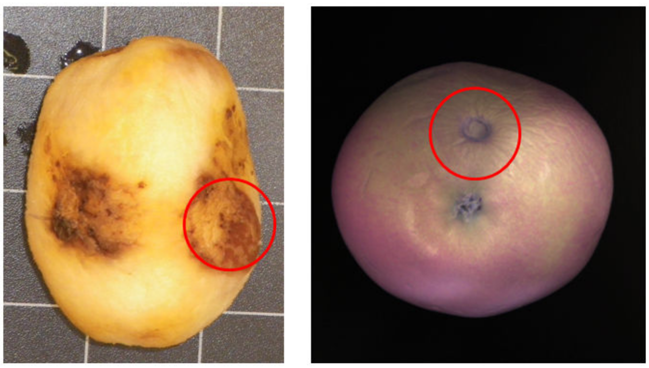

(a) (b)

Figure 3-10: Defect types: (a) Color defect (b) 3-dimensional defect

For contour extraction, first order edge detection operators (*Prewitt* edge detection operator, *Sobel* edge detection operator, *Canny* edge detection operator) and second order edge detection operators (*Laplace*, *Marr-Hildreth* operator) are always concerned. Reference [24] offers more detail about edge detection.

Classification of features for defects detection on agricultural products is quite demanding in general. The algorithms have to meet the expectations concerning the flexibility and adaptability. These requirements can be reached by application of supervised learning algorithms. In experiments several approaches are available: naive Bayes classifier, decision tree, artificial neural network, k-nearest neighbor (KNN), support vector machine (SVM).

SVMs were developed by Cortes and Vapnik [25] for binary classification. The basic idea of SVM is to maximize the margin between two classes with a constraint of, components of each classes locate on different sides of margin. In math, it can be described by following two equations:

$$\min \quad \frac{1}{2}\|w\|^2 + C\sum_{i=1}^{n}\zeta_i \;\; ; \quad i = (1,2,\dots,n)$$

$$\textit{subject to} \quad y_i[\langle w, x_i\rangle + b \geq 1 - \zeta_i] \;\; ; \quad \zeta_i \geq 0$$

where w is normal vector of hyperplane, C is soft margin parameter, ζ_i is penalized parameter, b is bias. In food industry, variant kinds of defects are possible. Therefore SVM can be adapted to multi-classification of defects. The following Fig. 3-11 illustrates classification of defects by using SVM algorithm.

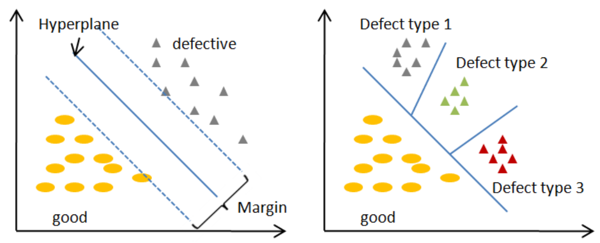

(a) (b)

Figure 3-11: Classification by using SVM: (a) classification of good and defective surface (b) further classification of defective surface; ellipsoid mark is feature vector indicating good surface, triangular mark is feature vector indicating defective surface.

K-nearest neighbor is another supervised learning algorithm, which can classify features based on closest training examples. Given a query feature, k (setting parameter) number of known feature closest to the query feature can be found. The classification is using majority vote among the k number of already classified features. K nearest neighbor algorithm used neighborhood classification as the prediction value of the new query feature. K number of nearest neighbor can be found by using Euclidean distance:

$$d_{q,k}^2 = (x_1^q - x_1^k)^2 + (x_2^q - x_2^k)^2 + \dots + (x_n^q - x_n^k)^2$$

where $d_{q,k}$ indicates the Euclidean distance between the query feature and the known feature, x_1^q indicates first element of query feature, x_1^k indicates first element of feature from known classification, et cetera. Fig. 3-12 illustrates classification of defects by using the KNN.

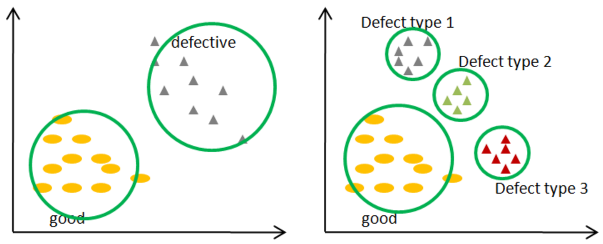

(a) (b)

Figure 3-12: Classification by using KNN: (a) classification of good and defective surface (b) further classification of defective surface; ellipsoid mark is feature vector indicating good surface, triangular mark is feature vector indicating defective surface.

Which feature is better to classify feature is a trade off. The answer to this question very much depends on the application and the specific classification. SVM methods are, in general, simpler and less computationally expensive, however week to address high dimensional feature. KNN can produce great results, however very computationally expensive due to its highly non-linear nature. Approximate classification algorithm can be developed by combining different supervised learning algorithms; interested reader can refer to [20].

IV. Geometric Path Planning

The issue of path planning has been studied for more than a few decades. The conventional approach for path planning is the application of the concepts of *configuration space* ($\mathcal{C}$-*Space*). In [26], the concept of *configuration space* and the *path planning algorithms* are clearly illustrated. The main challenge in path planning is to directly compute $\mathcal{C}_{obc}$ and $\mathcal{C}_{free}$, with often a quite high dimensionality of the $\mathcal{C}$-Space [27].

A geometric path planning algorithm proposed by in [28] will be introduced here. This algorithm has been proved to obviously reduce computation time and find a shortest collision-free path by utilizing the output of the computer vision module and by eliminating any extra work to model the workspace of the robot.

4.1 Workspace Representation

The 3D geometric path planning algorithm in which the *world* $\mathcal{W} = \mathbb{R}^3$ is based on distance transform where the workspace is modeled as a digital image with a set of occupiable cells as illustrated in Fig. 4.1. Each cell can either be free, occupied by an obstacle or occupied by a point on the path of the robot. Each cell is initialized to zero to indicate a free cell and then the *obstacle region* $\varphi \subseteq \mathcal{W}$ is systematically constructed by performing a one-time simple sequential scan of the workspace to assign a non-zero value to all cells occupied by obstacles. The free space $\mathcal{C}_{free}$ then becomes $\mathcal{W}$-φ [26].

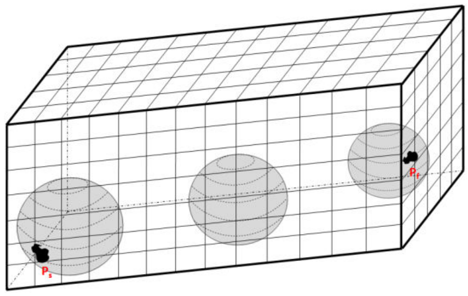

Figure 4-1: The 3D digital image of the workspace with 3D objects. The initial and final positions are notated by p_s and p_f respectively.

4.2 Path Planning Algorithm and Improvement

In 3D, each cell has 26 adjacent cells, while in 2D each cell has only 8 adjacent cells (see Fig. 4-2). Given the initial and final position of the end-effector, p_s and p_f, the path is computed by recursively re-evaluating the distance to the final goal from each of the neighboring cells to select the next intermediate cell that lies on the path.

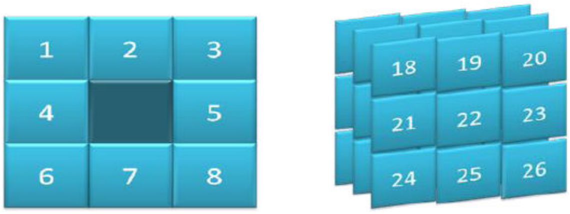

Figure 4-2: In 2D, each cell has 8 adjacent cells. In 3D, each cell has 26 adjacent cells. [26]

```
while ( distance ≥ ε):
    for i = 1 → 26:
        dist(i) = ∞
        if (cell(i) is free & !=history)
            dist(i)=norm( cell(i)- Pf )
    [distance I] = min(dist)
    new cell = cel(I)
```

At each iteration, the Euclidean distance from all the 8 adjacent cells to the final position is initialized to infinity and then reassigned the actual distance if the cell is not occupied by an obstacle and it is not already part of the path. Finally, the cell with the shortest distance from the goal is selected and added to the path. This process is repeated until the distance from the goal is less than the specified tolerance ε [26].

Some readers might argue that it is impossible to reach the goal position by utilizing the algorithm above; due to the goal position itself lies on the surface of obstacles (review Figure 4-1). Therefore, one improvement has to be done. In section 3, the coordinate of defect point detected by camera system should be offset from the surface of 3D objects with a distance of l_{offset}. Now, the algorithm can be employed in our paper. The shortest collision-free path is illustrated in Fig. 4-3.

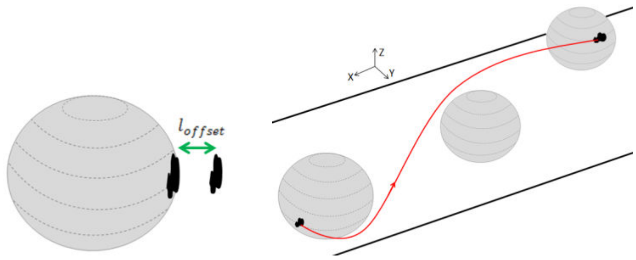

(a) *(b)*

Figure 4-3: (a) Defect point is offset from surface.
(b) Optimal path connecting the initial and goal position

Defect offset is a significant issue which determines the successful utilization of geometric path planning. How and how much is the goal position offset depends on the processing measures. In food industry there are two typical processing measures: milling directly on defect location along the centripetal direction or remove defects by water jet. These two measures are illustrated by Fig. 4-4. The red routes indicate the processing path.

For milling, a defect can be offset centrifugally, whereas for removing by water jet a defect can be offset somewhere spatially which is determined by removing strategy. Nevertheless, for both measures the condition has to be fulfilled in order to offset the defect location to a new and free cell: the distance of offset should be larger than the diagonal distance of a special cell illustrated in Fig. 4-1. If the special cells are cube, then the condition can be expressed by the following equation:

$$l_{offset} > \sqrt{3} \cdot l_{cell} \qquad (4.1)$$

l_{cell} is size of the cube cell.

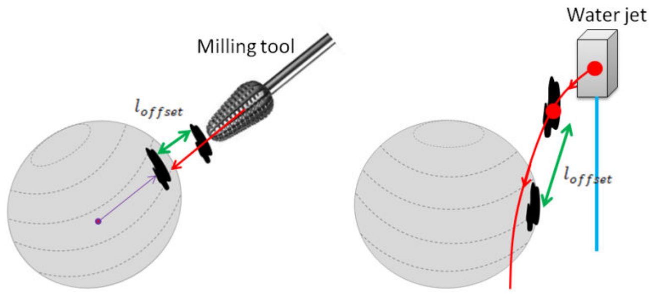

(a) (b)

Figure 4-4: Two example measures of processing in food industry: (a) milling along the centripetal direction (b) remove defects by water jet.

4.3 Application on Movable Objects

The geometric path planning algorithm has been proved to be efficient in real-time path planning, which can be incorporated in robot system with on-board sensors. This is quite important for industrial application on processing movable objects which is transported by a conveyor belt.

Figure 4-5 illustrates the industrial application of geometric path planning algorithm on moving objects. (a) End-effector is set to wait in the front of workspace, if the unprocessed objects don't appear in the workspace. (b) End-effector begins to move to an unprocessed object, if the unprocessed object containing defects appears in workspace. (c) After processing, the end-effector moves to next unprocessed object.

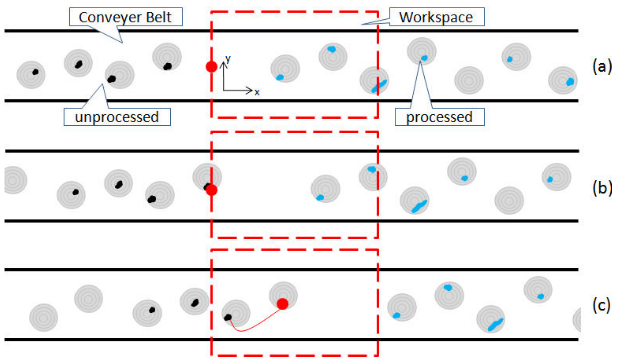

Figure 4-5: Application on movable objects which are conveyed from left to right. Red spot: Position of end-effector; Blue spot: processed object; Black spot: unprocessed object

In order to process moving objects, in a way as they were unmoved, the velocity of moving objects should be taken into account. The conveying velocity should be supplemented to the velocity of processing tool (milling tool or water jet).

V. Realization and Implementation

The definition of specific problem has to be considered for the conceptualization of processing and machine design. In addition to the geometry of objects and characteristic of defects, the processing speed and accuracy also have to be considered. For flat products a two axes portal frame might be sufficient. Objects with a more complex geometry need a machine design with an appropriately increased number of degrees of freedom.

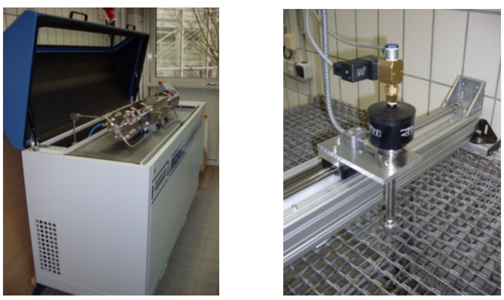

Figure 5-1: Test facility for water jet cutting

Corresponding to different inspected goods there are different method for processing. For example, water jet cutting is particularly suitable for food processing and a flexible and fast processing method (Fig. 5-1).

The analysis of acquired image data is performed by an implemented software solution (Fig. 5-2).

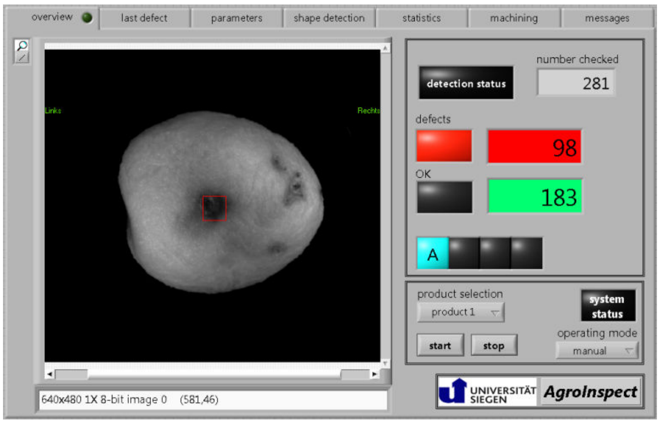

Figure 5-2: GUI example of a software for automated defect detection

VI. Conclusion

In this paper, approaches for defect detection and geometry estimation were discussed. Based on these approaches an algorithm and application for path planning were also presented. A comparison of several computer vision methods has been performed. As a result the choosing of a suitable principle for defects detection and shape recognition will be facilitated according to the performed survey.

Specific processing of defects for example on agricultural objects helps to reduce the waste. For this surface defects detection and geometry estimation have to be combined to deduce the processing method and the path planning. Application of the presented methodology depends on the specific problem definition. Vision guided applications could be conceptualized by this universal methodology.

The aim of this paper was to present approaches for surface inspection, geometry estimation and path planning. This facilitate the selection of a suitable approach for a specific task. Sensor guided processing can be found in various applications. Machine concepts for such application could be adapted faster.

References

[1] R. Lu, B. Park, "Hyperspectral and multispectral imaging for food quality and safety," in *Sensing and Instrumentation for Food Quality and Safety*, Jg. 2, pp. 131-132, 2008.

[2] M. Michelsburg, R. Gruna, K.-U. Vieth, F. Puente Léon, "Spektrale Bandselektion beim Entwurf automatischer Sortieranlagen," in *Forum Bildverarbeitung 2010*. KIT Scientific Publishing, 2010, pp. 389-400.

[3] M. Weyrich, P. Klein, M. Laurowski, "Optische Lokalisierung, Klassifizierung und automatische Behebung von Fehlern am Beispiel von Agrarprodukten," in *Forum Bildverarbeitung 2010*. KIT Scientific Publishing, 2010, pp. 389-400.

[4] M. Weyrich, P. Klein, M. Laurowski, Y. Wang, "Vision based Defect Detection on 3D Objects and Path Planning for Processing", *Proceedings of the 9th WSEAS International Conference on ROCOM*, WSEAS Press, 2011.

[5] T. Brosnan, D.-W. Sun, "Inspection and grading of agricultural and food products by computer vision systems a review," in *Computers and Electronics in Agriculture*, Jg. 36, H. 2-3, pp. 193-213, 2002.

[6] T. Kerstein, M. Laurowski, P. Klein, M. Weyrich, H. Roth, J. Wahrburg, "Optical 3D-Surface Reconstruction of Weak Textured Objects Based on an Approach of Disparity Stereo Inspection," in *ICPRCV 2011, "International Conference on Pattern Recognition and Computer Vision*", submitted for publication.
[7] S.-J. Huang, F.-r. Ying, "Stereo Vision Image Processing Strategy for Moving Objects Detection," in *Sensors, Signals, Visualization, Imaging, Simulation & Materials,* WSEAS Press, 2009, pp. 127-132.
[8] O. Demuynck, C. P. Cedeno, A. L. Moore, "Industrial Machine Vision System for Fast and Precise 3D Object Localization," in *Proceedings of the 9th WSEAS International Conference on Signal Processing, Computational Geometry and Artificial Vision, 2009, pp. 160-164.*
[9] D. Scarpin, J. Wahrburg, "Entwicklung eines robotergeführten Lichtschnittsensors für die berührungslose Erfassung anatomischer Strukturen," in *O. Burgert, A. K. Lüder, B. Preim, J. Schipper, (Ed.) 9. Jahrestagung der Deutschen Gesellschaft für Computer- und Roboterassistierte Chirurgie e.V.*, DAV Verlag pp. 231-235, 2010.
[10] P. Besl, "Active Optical Range Imaging Sensors," in *Machine Vision and Applications*: Springer, Bd. 1, 1998. pp. 127-152.
[11] N. Lazaros, G. C. Sirakoulis, A. Gasteratos, "Review of Stereo Vision Algorithms: From Software to Hardware," in *International Journal of Optomechatronics*, Jg. 2, H. 4, pp. 435-462, 2008.
[12] R. Zhang, P.-S. Tsai, J. E. Cryer, M. Shah, "Shape from Shading: A Survey," in *IEEE Transactions on Pattern Analysis and Machine Intelligence*, Jg. 21, PP. 690-706, 1999.
[13] R. Calow, "Schnelles Zeilensensorsystem zur gleichzeitigen Erfassung von Farbe und 3D-Form," in *Forum Bildverarbeitung 2010*. KIT Scientific Publishing, 2010, PP. 181-192.
[14] H. Hamfeld, *Aktive Stereoskopie*, Univ. Kaiserslautern, Germany, Fachbereich Informatik, 2002.
[15] D. Modrow, *Real-time active stereoscopic system for technical and biometric application*, TU Munich, Germany, 2009.
[16] G. Gao, X. Chen, H. M. Zhang, "A Fast Structured Light Matching Method in Robot Stereo Vision," in *Journal Applied Mechanics and Materials*, vol. 29 - 32, pp. 1981-1984, 2010.
[17] K. Ambrosch, W. Kubinger, "Accurate hardware-based stereo vision," in *Journal of Computer Vision and Image Understanding*, vol. 114, issue 11, Elsevier Science, New York, NY, 2010.
[18] G. Xu and B. Liu, "A Mesh-candidate-based 3D Reconstruction System for Online Depth Recovery," in *2nd International Conference on Computer Engineering and Technology (ICCET), 2010*, pp. 257-268, 2009.
[19] C.-M. Pun, C. Li, "Shape Classification Using Simplification and Tangent Function" in *Proceedings of the 8th WSEAS International Conference on Circuits, Systems, Electronics, Control & Signal Processing (CSECS '09), 2009, pp. 261-266.*
[20] O. Kissing, *Ein Beitrag zur Gestaltung einer lernfähigen Klassifikation in der automatischen Oberflächeninspektion*, Diss. Universität Siegen, Shaker, Aachen 2010.
[21] W. R. Stevenson, *Compendium of Potato Diseases,* 2. ed., 3. printing. St. Paul, Minn.: APS Press, 2009.
[22] A. Ligocki, *Schneiden landwirtschaftlicher Güter mit Hochdruckwasserstrahl*, Techn. Univ., Diss.-Braunschweig, Aachen: Shaker, 2005.
[23] M. Fuß, *Verfahren zur Automatisierung der visuellen Oberflächeninspektion mit Hilfe der Bildverarbeitung*, Universität Siegen, Dissertation, 1997.
[24] M. Nixon; A. Aguado, *Feature Extraction & Image Processing*, Second edition; Elsevier Ltd., 2008.
[25] C. Cortes, V. Vapnik, "Support-vector network," *Machine Learning*, 20,1-25; 1995
[26] S. M. LaValle, *Planning Algorithms*, Cambridge University Press. 2006.
[27] B. Siciliano, O. Khatib, *Handbook of Robotics*, Springer, 2008.
[28] Z. Aljarboua, "Geometric Path Planning for General Robot Manipulators," WCECS 2009.
[29] V. Niola, C. Rossi, S. Savino, S. Strano, "Robot Trajectory Planning by Points and Tangents," in *Proceedings of the 10th WSEAS Int. Conference on ROCOM*; WSEAS Press, 2010.
[30] Y. Zhang, J. Wang, "Obstacle Avoidance for Kinematically Redundant Manipulators Using a Dual Neural Network," in *Proceedings of the 8th WSEAS Int. Conference on ROCOM*; WSEAS Press, 2008.